The Effect of Particle Concentration of Poly(*p*-phenylene) on Electrorheological Response

JEONG-IN SOHN,[1] JUN H. SUNG,[2] HYOUNG J. CHOI,[2] MYUNG S. JHON[3]

[1] Department of Chemistry, Hallym University, Chunchon 200-702, Korea

[2] Department of Polymer Science and Engineering, Inha University, Inchon, 402-751, Korea

[3] Department of Chemical Engineering, Carnegie Mellon University, Pittsburgh, PA 15213

Received 15 July 2001; accepted 12 September 2001

ABSTRACT: Poly(*p*-phenylene) (PPP) particle-based electrorheological (ER) fluids were prepared from $FeCl_3$-doped PPP and silicone oil. The effect of the volume fraction of PPP and applied electric field strength on ER response was investigated via measured rheological properties, including flow curve, shear viscosity, and yield stress. Furthermore, the yield stresses of the PPP-based ER fluid, which exhibit the typical characteristics of a Bingham fluid, were measured. The yield stress data collapse on a universal scaling function proposed by Choi et al. © 2002 Wiley Periodicals, Inc. J Appl Polym Sci 84: 2397–2403, 2002

Key words: electrorheological fluid; poly(*p*-phenylene); rheology; yield stress; suspension

INTRODUCTION

Electrorheological (ER) fluids, which are the suspensions of micron-sized polarizable particles dispersed in nonconducting liquids, are fascinating materials whose suspension microstructure and rheological properties, including yield stress and viscosity, are dramatically altered by external electric fields.[1,2] The dramatic increase in viscosity and rapid response time originate from the substantial alteration of the suspension structure, especially the field-induced formation of fibrous aggregates aligned with the electric field. Polarized particles behave as electric dipoles, which attract each other to form chain and column structures aligned along the external field direction,[3] and all of the physical and mechanical properties of the suspensions induced by the applied electric field are reversible.[4,5]

A wide variety of particulate materials were employed in ER suspensions, including starch, flour, silica, alumina, titania, zeolite, and semiconducting polymers. Among these, the conventional hydrous ER particles are known as wet-base systems (e.g., starch, silica, alumina, and titania), which require a small amount of water or some other polar molecule as an additive or promoter. The wet-base system has severe limitations in its engineering application, including thermal instability, water evaporation, corrosion of device, and so on.[6–8] Recently developed dry-base systems also exhibit the strong ER characteristics; intrinsic charge carriers in either bulk particles or their surfaces move locally under the applied electric field to generate a field-induced structure with polarized particles. The ER fluid based on a semiconducting polymer is one of the novel, intrinsic ER systems. The anhydrous ER materials are polarizable with conducting and

Correspondence to: H. J. Choi (hjchoi@inha.ac.kr).
Contract grant sponsor: Hallym Academy of Sciences.

Journal of Applied Polymer Science, Vol. 84, 2397–2403 (2002)
© 2002 Wiley Periodicals, Inc.

electroluminescent material, including polyaniline,[9,10] copolystyrene particles with a polyaniline coating,[11] poly(aniline-*co*-*o*-ethoxyaniline),[12] poly(acenequinone) radicals,[13] and poly(*p*-phenylene) (PPP).[14] On the other hand, continuous phases, including silicone and hydrocarbon oils, possess low conductivity and large dielectric breakdown strength.

The electrostatic polarization mechanism was known to result in the field-induced polarization of the disperse phase particles relative to the continuous phase,[15] in which the driving force of the particle fibrillation originates mainly from the electrostatic interaction between particles. The dielectric constant mismatch between the particles and the dispersing oil causes this interaction.[16] Overlap of electric double layers[17,18] in the particle has also been suggested as a potential mechanism for ER response. Each particle is surrounded by a diffuse counter ion cloud, which distorts and overlaps with neighboring counter ion clouds and enhances the electrostatic repulsion among particles.[19]

The PPP in general is a simple conjugated polymer consisting of phenylene rings and is an insoluble and infusible dark brown material with low electric conductivity. This material was one of the first reported to have blue electroluminescence.[20,21] Plocharski et al.[22] pointed out that ER characteristics are determined primarily from the ionic polarizability and the ion movement in the suspended particle material. They investigated the PPP with anhydrous ferric chloride $FeCl_3$ dissolved in dry nitromethane and then observed the increase in the ER effect with increasing dielectric constant.

EXPERIMENTAL

Semiconducting PPP particles were synthesized by adopting the procedure of Kovacic and Oziomek.[23] PPP, which provides mechanical and chemical stability, was synthesized via simple bulk polymerization of benzene (Daejung Chemical, Inchon, Korea).[24] PPP particles were doped with 5 wt % $FeCl_3$ (Kanto Chemical, Tokyo, Japan) in aqueous solution to increase electric conductivity. Recently, functional PPP was also synthesized by using palladium catalyst.[25] In most cases, the synthesized PPP particles do not contain more than 10 repeat units[26] because of (1) the occurrence of side reactions, which destroy functional groups and suppress further chain growth, and (2) the occurrence of product precipitating from the solution.[27]

In this article, the benzene was converted to PPP by using cupric chloride ($CuCl_2$; Aldrich, Milwaukee, WI) in a nitrogen environment. The polymerization temperature was kept at 45°C. A reaction involves formation of the intermediate dihydro units via a series of electron and proton transfers. At an early stage in the reaction, water was added as an initiator and the stirring speed was maintained at approximately 400–500 rpm for 2 h. After polymerization, the mixture was washed with water and ethyl alcohol to remove CuCl and aqueous acid. The chemical reaction diagram of PPP is as follows:

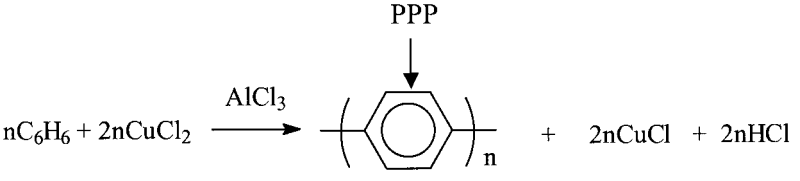

In the oxidative coupling process, PPP is also generated by electrochemical coupling,[28] which is known to produce a phenolic unit and is more feasible for electron-rich monomers, including thiophene and pyrrole. The PPP was then dried and milled. To increase conductivity, the PPP particle was doped with $FeCl_3$ aqueous solution for 48 h at 25°C. After doping, the PPP particles were filtered and dried. The ER fluids with PPP particles dispersed in silicone oil were prepared by suspending the mixture at 1500–1800 rpm by using Pearl Mill (Shinil Co., Korea). Before suspending the PPP particles in the oil, the particles were dried for 1 day. The kinematic viscosity and the density of the silicone oil were 30 cS and 0.960 g/cm^3, respectively.

To examine the chemical structure of the synthesized PPP, FTIR spectroscopy (Bruker IFS 48, Ettlingen, Germany) was used. Particle sizes and their distributions were measured by a particle size analyzer (Malvern MS 20, Malvern, U.K.); particle shape was measured by a scanning elec-

tron microscope (SEM S-2400, Hitachi, Hitachnaka, Japan), and the density of the PPP was measured with a pycnometer. Density of the PPP particle was 1.21 g/cm^3. In the conductivity measurements, the picoammeter (Keithley 487, Cleveland, OH) with a custom-made cell (two probes) was used to measure pellets of each sample. Two different voltages (10 and 100 V) were applied and the corresponding currents (I) were measured.[29,30] The conductivity σ was then calculated from the equation[31]

$$R = \frac{V}{I} = \frac{d}{\sigma A} \tag{1}$$

where A is the surface area and d is the thickness. The samples were indexed to be PPP-1, PPP-2, PPP-3, and PPP-4 for 2.40, 4.01, 5.64, and 8.10 vol % of the PPP in silicone oil, respectively.

Electrorheological properties of the PPP-based ER fluids were measured by using a rotational rheometer (Physica MC120, Stuttgart, Germany) with a Couette geometry (Z3-DIN) equipped with a high-voltage generator (HVG 5000, Stuttgart, Germany). Temperature was controlled by a circulating oil bath (Viscotherm VT100). Several DC electric field strengths (1–3.5 kV/mm) were applied to the insulated bob. The yield stress was then measured from both controlled shear rate (CSR) mode, which is the value of the flow resistance at the shear rate presetting, and controlled shear stress (CSS) mode determined by presetting the shear stress and recording the shear rate.

RESULTS AND DISCUSSION

The PPP-based ER fluid in this study is of technological interest because of its high stability and relatively easy control of doping at low concentrations. Figure 1 shows the FTIR spectra of the PPP particle, showing a strong peak at 800 cm^{-1} for the C—H out-of-plane deformation of 1,4-distributed benzene, a peak at 1033 cm^{-1} for in-plane deformation, and peaks at 1403 and 1478 cm^{-1} for the ring-stretching structure. The particle size distribution of the synthesized PPP was measured in the range of 15–25 μm (in diameter). The shape was irregular for both the doped and the undoped particles.

A synthesized PPP particle shows semiconducting behaviors with moving charge carriers that can be activated under a strong applied electric field. It is known that certain polymers including PPP are highly conductive in the presence of dopants that are electron acceptors, such as pentafluoride and halogen, or electron donors, such as alkali metals. The conductivity varies with dopant concentration and doping may affect the rearrangement of charges in polymer backbone.[32] However, interchain transport of electrons in doped PPP, due to the charged defect structure, could be intensified upon application of the external field. There exists conductivity change due to the degree of doping. Doped PPP leads to increased conductivity. For example, undoped and 5.0 wt % doped with $FeCl_3$ have conductivities of 1.12×10^{-13} and 4.40×10^{-10} S/cm, respectively.

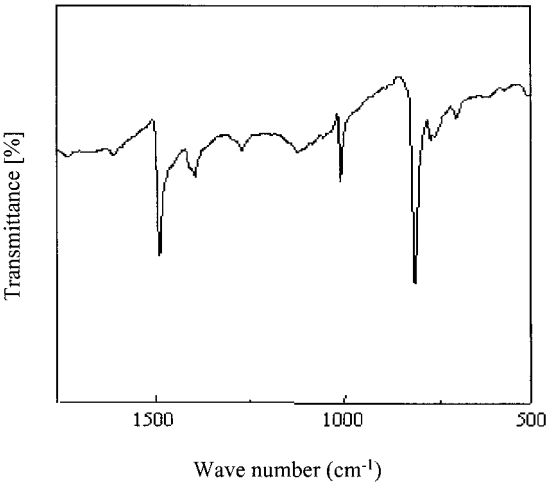

Figure 1 FTIR spectra of PPP.

The rheological properties of an ER fluid vary when an electric field is imposed by forming a characteristic fibrillation structure, with strings of particles oriented along the electric field direction. Figures 2 and 3 show the flow curves for shear stress and shear viscosity versus shear rate, respectively, via CSR test at five different electric field strengths (0, 1.0, 2.0, 3.0, and 3.5 kV/mm). In the absence of an electric field, the suspension behaves similar to an ordinary suspension. However, when the electric field is applied, the shear stress and shear viscosity at a given shear rate increase with electric field strength. The shear stress initially decreased with shear rate and then increased at the point of breaking, as shown in Figure 2. At the lower shear rate, the fibrillated structure uniformly deformed initially, but after a few minutes, a zone devoid of fibrils developed in the middle of the gap, and shearing from then on took place for the most part in the central region. An electrohydro-

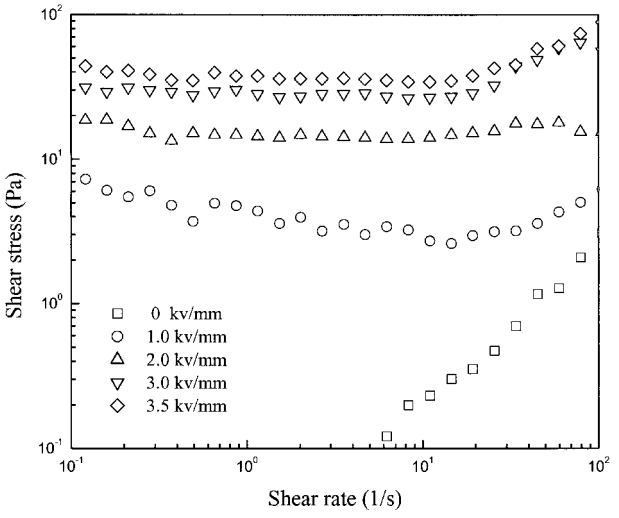

Figure 2 Shear stress versus shear rate of PPP-3 for various electric field strengths at 25°C.

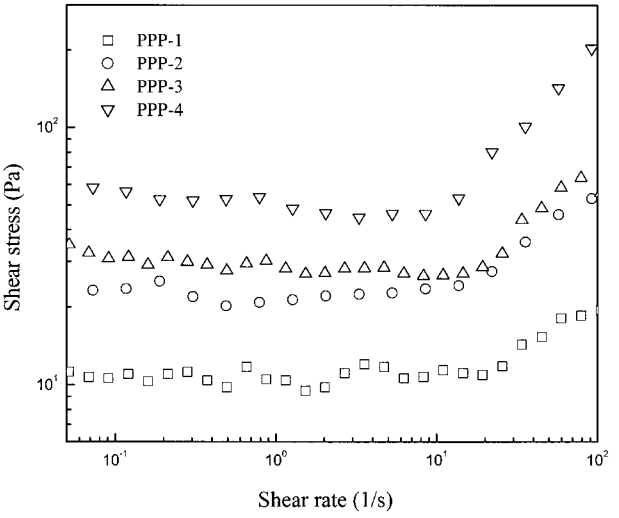

Figure 4 Shear stress versus shear rate for PPP-1, PPP-2, PPP-3, and PPP4 under the electric field strength of 3 kV/mm at 25°C.

dynamic effect occasionally occurred, particularly at high electric field strengths, destroying the fibrillated structure. At the higher shear rates, the fluid motion was more chaotic and the formation of the zone without fibrils in the central region was not well defined.[33] Figures 4 and 5 show shear stress and shear viscosity from a CSR test for four different fractions under electric field strengths of 3.0 kV/mm. Both the shear stress and the shear viscosity of doped PPP suspensions increase with volume fraction.[34,35] Generally, the structure in a concentrated suspension can be sufficiently rigid to permit the material to withstand a certain level of deforming stress without flowing. The maximum stress that can be sustained without flow is defined as yield stress.

Figure 6 indicates the dependence of yield stress (τ_y) on electric field strength (E) for various volume fractions of PPP suspensions via CSR. As expected, the yield stress increases with both particle concentration and electric field strength because of an increase in the polarization forces among particles.[36] Figure 7 shows that viscosity changes with the volume fraction in various electric field strengths.

Figure 8 shows the yield stress for four different PPP volume fractions. The static yield stress

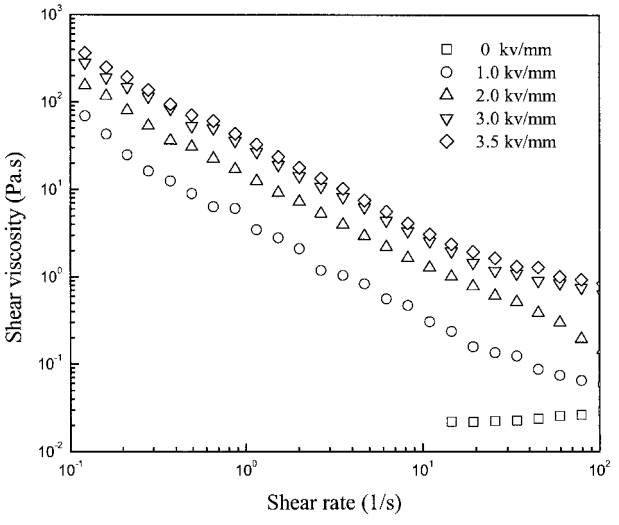

Figure 3 Shear viscosity versus shear rate of PPP-3 under various electric field strengths at 25°C.

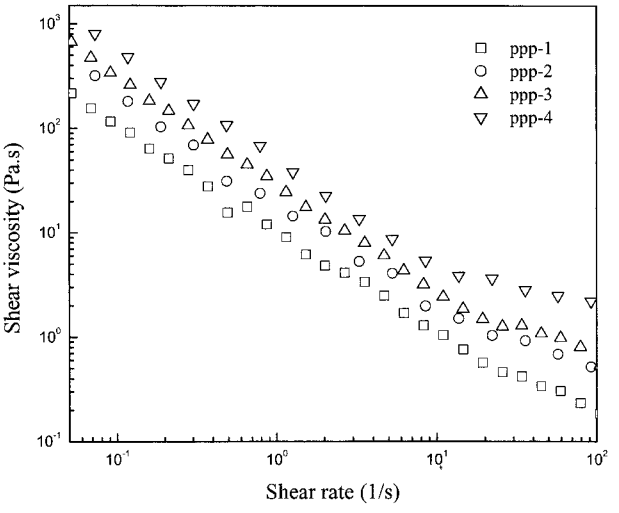

Figure 5 Shear viscosity versus shear rate for PPP-1, PPP-2, PPP-3, and PPP-4 under the electric field strength of 3 kV/mm at 25°C.

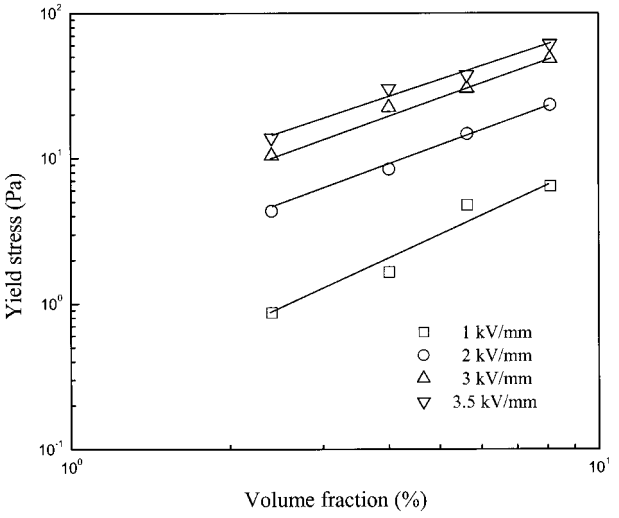

Figure 6 Yield stress versus volume fraction for various electric field strengths.

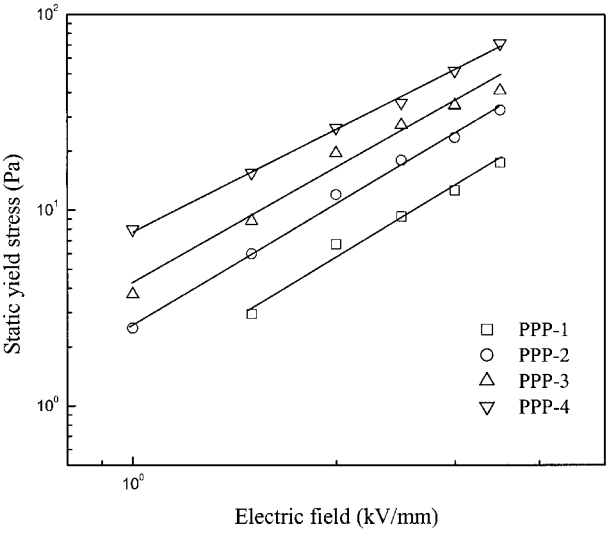

Figure 8 Yield stress versus electric field strength for four different PPPs with 5 wt % doping of $FeCl_3$ at 25°C.

from a CSS test was performed for the PPP suspensions with six different electric field strengths (1.0, 1.5, 2.0, 2.5, 3.0, 3.5 kV/mm). As the volume fraction of doped PPP increases, the yield stress increases exponentially. The PPP-based ER fluids behave similar to power-law fluids with a power-law of −1. The correlation between yield stress and electric field strength is represented. The yield stress is also enhanced by increasing the volume fraction. Generally, the correlation of the yield stress and electric field was presented as follows:

$$\tau_y \propto E^m \tag{2}$$

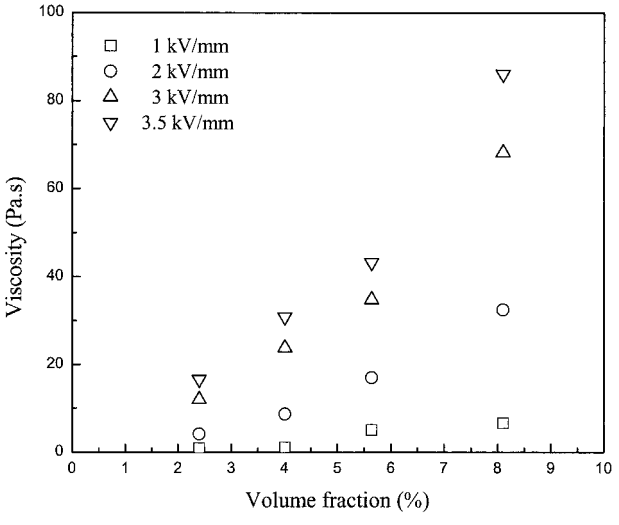

Figure 7 Shear viscosity versus volume fraction for various electric field strengths.

The m values for the PPP series were 2.0, 2.0, 1.96, and 1.73, respectively. The dependency of the yield stress on the electric field strength differs from the E^2 dependency suggested by the polarization model.[37] The applied electric field induces electrostatic polarization interactions among the particles and also between the particles and the electrodes.

However, the conduction model does not describe the flow effect accurately; that is, ER response is influenced by the conductivity mismatch and the interaction between particle and medium. Various ER fluids show different exponents in eq. (2). A correlation between yield stress and electric field strength is represented in Figure 9. To correlate yield stress with the broad range of electric field strengths, Choi et al..[38] introduced the universal yield stress equation

$$\tau_y(E_0) = \alpha {E_0}^2 \left(\frac{\tanh \sqrt{E_0/E_c}}{\sqrt{E_0/E_c}} \right) \tag{3}$$

where α depends on the dielectric constant and the particle volume fraction, and E_c is the critical electric field strength, which is proportional to the particle conductivity. By the normalized scaling function,[38]

$$\hat{\tau} = 1.313 \hat{E}^{3/2} \tanh \sqrt{\hat{E}} \tag{4}$$

where $\hat{E} = E_0/E_c$ and $\hat{\tau} \equiv \tau_y(E_0)/\tau_y(E_c)$. The PPP data are collapsed onto a single curve by using eq.

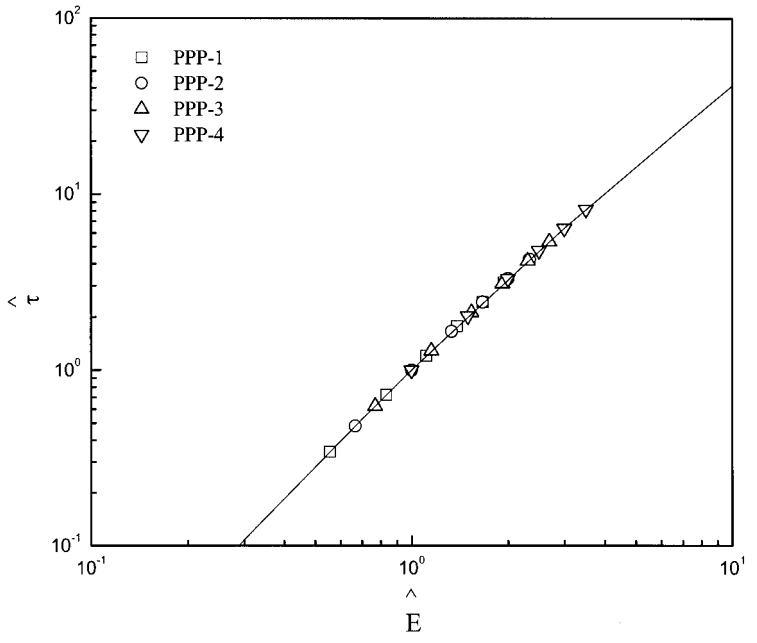

Figure 9 The universal curve for $\hat{\tau}$ versus $\hat{E}$ for four different PPPs.

(4), which is shown in Figure 9. E_c's for the four PPP volume fractions are 1.8, 1.5, 1.3, and 1.0 kV/mm, respectively.

CONCLUSION

The ER fluids of PPP for four different volume fractions in silicone oils show an increase in the apparent viscosity under the electric field strengths. The shear stress and shear viscosity increased with electric field strength and volume fraction. The yield stress of the doped PPP-based suspension increased with volume fraction and correlated very well with the universal scaling curve proposed by Choi et al.[38]

This work was supported by Hallym Academy of Sciences, Hallym University, Korea (2001).

REFERENCES

1. Tao, R.; Sun, J. M. Phys Rev Lett 1991, 67, 398.
2. Trlica, J.; Sáha, P.; Quadrat, O.; Stejskal, J. Physica A 2000, 283, 337.
3. Gulley, G. L.; Tao, R. Phys Rev E: Stat Phys, Plasmas, Fluids, Relat Interdiscip Top 1997, 56, 4328.
4. Wu, S.; Lu, S; Shen, J. Polym Int 1996, 41, 363.
5. Kim, J. W.; Choi, H. J.; Lee, H. G.; Choi, S. B. J Ind Eng Chem 2001, 7, 218.
6. Sprecher, A. F.; Carlson, J. D.; Conrad, H. Mater Sci Eng 1987, 95, 187.
7. Uejima, H. J Appl Phys 1972, 11, 319.
8. Conard, H.; Sprecher, A. F.; Choi, Y.; Chen, Y. J Rheol 1991, 35, 1393.
9. Kim, S. G.; Kim, J. W.; Cho, M. S.; Choi, H. J.; Jhon, M. S. J Appl Polym Sci 2001, 79, 108.
10. Lee, J. H.; Cho, M. S.; Choi, H. J.; Jhon, M. S. Colloid Polym Sci 1999, 277, 73.
11. Kuramoto, N.; Yamazaki, M.; Nagai, K.; Koyama, K.; Tanaka, K.; Yatsuzuka, K., Higashiyama, Y. Rheol Acta 1995, 34, 298.
12. Choi, H. J.; Kim, J. W.; To, K. Synth Met 1999, 101, 697.
13. Choi, H. J.; Cho, M. S.; Jhon, M. S. Int J Modern Phys B 1999, 13, 1901.
14. Vaschetto, M. E.; Monkman, A. P.; Springborg, M. J Mol Struct Theochem 1999, 468, 181.
15. Parthasarathy, M.; Klingenberg, D. J. Mat Sci Eng 1996, R17, 57.
16. Halsey, T. C. Science 1992, 258, 761.
17. Klass, D. L.; Martinek, T. W. J Appl Phys 1967, 38, 67.
18. Klass, D. L; Martinek, T. W. J Appl Phys 1967, 38, 75.
19. Weiss, K. D.; Carlson, J. D.; Coulter, J. P. J Intellect Mater Sys Struct 1993, 4, 13.
20. Grem, G.; Leditzky, G.; Ullrich, B.; Leising, G. Adv Mater 1992, 4, 36.

21. Grem, G.; Martin, V.; Meghdadi; F., Paar, C.; Stampfl, J.; Sturm, J.; Tasch, S.; Leising, G. Synth Met 1995, 71, 2193.
22. Plocharski, J.; Rozanski, M.; Wycislik, H. Synth Met 1999, 102, 1354.
23. Kovacic, P.; Oziomek, J. J Am Chem Soc 1962, 85, 454.
24. Sim, I. S.; Kim, J. W.; Choi, H. J.; Kim, C. A.; Jhon, M. S. Chem Mater 2001, 13, 1243.
25. Chung, D. J.; Bae, J. Y. J Ind Eng Chem 1999, 5, 290.
26. Kovacic, P.; Jones, M. B. Chem Rev 1987, 87, 357.
27. Schlûter, A. D.; Wegner, G. Acta Polym 1993, 44, 59.
28. Rubinstein, I. Electrochem Soc 1983, 130, 1506.
29. Lee, J. M.; Lim, K. H. J Ind Eng Chem 2000, 6, 157.
30. Park, S. H.; Kwon, T. Y. J Ind Eng Chem 2000, 6, 226.
31. Choi, H. J.; Lee, J. H.; Cho, M. S.; Jhon, M. S. Polym Eng Sci 1999, 39, 493.
32. Chance, R. R.; Brédas, J. L.; Silbey, R. Phys Rev B: Solid State 1984, 29, 4491.
33. Choi, H. J.; Cho, M. S.; Kang, K. K.; Ahn, W. S. Micropor Mesopor Mater 2000, 39, 19.
34. Kim, J. W.; Choi, H. J.; Yoon, S. H.; Jhon, M. S. Int J Mod Phys B 2001, 15, 634.
35. Choi, H. J.; Kim, J. W.; Suh, M. S.; Shin, M. J.; To, K. Int J Mod Phys B 2001, 15, 649.
36. Kim, J. W.; Kim, S. G.; Choi, H. J.; Suh, M. S.; Shin, M. J.; Jhon, M. S. Int J. Mod Phys B 2001, 15, 657.
37. Klingenberg, D. J.; van Swol, F.; Zukoski, C. F. J Chem Phys 1991, 94, 6170.
38. Choi, H. J.; Cho, M. S.; Kim, J. W.; Kim, C. A.; Jhon, M. S. Appl Phys Lett 2001, 78, 3806.